

THE TALE OF THE HIDDEN SHAFT

Luca G. Zarotti

*Institute for Agricultural and Earthmoving Machinery of the Italian National Research Council, Ferrara, Italy
gl.zarotti@imamoter.cnr.it*

Abstract

The paper addresses the combination of two or more volumetric machines (pump/motor) connected by a shaft without any external links, defined here by as CSU (Cross Shaft Unit). In the first part, the CSUs are classified in three groups (Type A, B and C) to discuss their general characteristics and field of application. In the second part, the focus is put on the Type C units, i.e. the so called rotational regenerative units, by analyzing their steady state and dynamic performance in a simulation environment to demonstrate the use of a model of the pump/motor losses and a tentative control system.

Keywords: fluid power, volumetric machines, energy, simulation

1 Introduction

How to decide if a fluid power device is original? The simplest method is to check it up on a definition. A reference book gives the following three definitions of the adjective original (Hornby, 1974): “¹first or earliest... ²newly formed or created... ³able to produce new ideas...” The first and second criterion share two weaknesses: firstly, they are more focused on time rather than quality; secondly, they might be difficult to proof or confirm because the technical birthright is often a disputable attribute. Conversely, the third criterion is more attractive in theory and more effective in practice because it’s focused on quality, open to the future and easy to verify.

A striking example of originality in this sense is the load-sensing concept, that was successful for several decades and still prompts new variants and improvements (Zarotti, 2001 and Leati et al., 2010). Within a less sophisticated context, the paper claims that the idea of connecting two or more volumetric machines by means of an internal shaft (i.e. without any mechanical links with the world outside), though simple and not new, opens a broad range of functional opportunities and legitimates its originality in full sense.

Actually, the above idea is applied here and there at various levels of complexity in fluid power applications but it lacks a unified view and, consequently, lacks a collective designation. The latter gap is readily recovered by naming CSU (Cross Shaft Unit) the pieces of

hardware where the idea is exploited; the former, i.e. the investigation of the topical features of the CSUs, is the matter of the first part of the paper. The second part is focused on the particular class that is convertible into the so called regenerative test circuits.

2 Classification and Definitions

The CSU concept generates three groups or classes of basic systems - Type A, B and C - with different functional properties and fields of applications. A combination of the basic systems is labeled as Type X.

2.1 Type A class

The CSU Type A class is generated by the common shaft specification only, free from any additional restrictions. The relevant schematic is shown in Fig. 1 where n volumetric machines (the CSU members) are connected by a single shaft and their $2n$ hydraulic ports are independent, i.e. each member belongs to a separate circuit. The volumetric displacement of all members is variable but variable and fixed members can be mixed or even all members can be fixed. The direction of the fluid flow is the same through all members (up or down).

This manuscript was received on 8 December 2010 and was accepted after revision for publication on 1 November August 2011

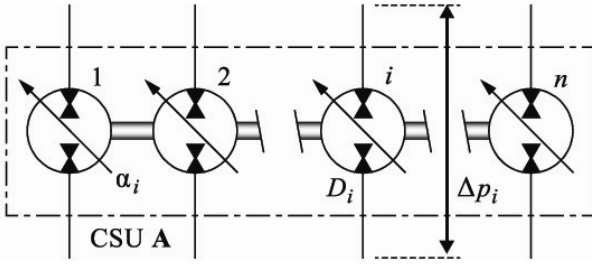


Fig. 1: Schematic of the CSU Type A class

$$M_i = D_i \cdot \alpha_i \cdot \Delta p_i - D_i \cdot \Delta p_{w,i} \quad \begin{cases} \Delta p_{w,i} > 0 \\ \alpha_i > 0 \end{cases} \quad (1)$$

The torque transmitted by the generic CSU member to the shaft is expressed by the general relationship three working modes are possible, as shown in Working modes according to at constant setting and speed:

- if $\alpha_i \Delta p_i > \Delta p_{w,i}$ the member works as a motor and the torque it transmits is positive;
- if $\alpha_i \Delta p_i < 0$ the member works as a pump and the torque it transmits is negative;

if $0 \leq \alpha_i \Delta p_i \leq \Delta p_{w,i}$ the member works as a power sink; in fact, seen from the shaft it would be a pump (because M_i is negative) but seen from the hydraulic ports it would be a motor (because Δp_i is positive). The extreme points or states A and B of this intermediate range are $\Delta p_i = 0$ (a neutral member) on the left and $M_i = 0$ (a idling member) on the right.

If the rotational speed is constant, the steady state operation requires that the overall shaft torque be balanced or

$$\sum_{i=1}^n D_i \cdot [\alpha_i \cdot \Delta p_i - \Delta p_{w,i}] = 0 \quad (2)$$

In principle, Eq. 2 is compatible with several combinations but some are purely speculative, e.g. one member working in the motor mode and the others in the sink mode or all members working in the idling state. A reasonable screening leads to a couple of pragmatic rules.

The first rule states that some members work as pumps and some others work as motors (first CSU rule). By rearranging the terms of Eq. 2, the result is

$$\sum_{i=1}^n D_i \cdot \alpha_i \cdot \Delta p_i = \sum_{i=1}^n D_i \cdot \Delta p_{w,i} \quad (3)$$

which proves that the unit as a whole appears a single idling motor (second CSU rule).

A corollary of the first rule is that at least one member works as a pump and at least one member works as a motor. This is the reason why the case of $n = 2$ is so important in some applications.

The flow rates through the volumetric members are also influenced by the common shaft. Their general expression is not unique because, apart from the assumption that no flow be exchanged between two adjacent members, two options apply to the drains. According to the first, all drains are internal, and the flow rate - the same in the input and output port - is the following

$$Q_{a,i} = Q_{b,i} = D_i \cdot \alpha_i \cdot \omega + \frac{\text{sgn}(\Delta p_i) + 1}{2} \cdot D_i \cdot \omega_{w,i} \quad (4)$$

where $\omega_{w,i}$ is the equivalent speed loss (i.e. the total flow loss divided by the displacement) and is always positive. According to the second, all drains are external and the input and output flow rates are different

$$\begin{cases} Q_{a,i} = D_i \cdot \alpha_i \cdot \omega + \frac{\text{sgn}(\Delta p_i) + 1}{2} \cdot D_i \cdot \omega_{w,i} \\ Q_{b,i} = D_i \cdot \alpha_i \cdot \omega + \frac{\text{sgn}(\Delta p_i) - 1}{2} \cdot D_i \cdot \omega_{w,i} \end{cases} \quad (5)$$

Equation 4 and 5 cover all operating modes of a generic member and, though depicting two extreme models, are good enough for broad range estimations.

The relationships involving torque and flow reduce the functional degrees of freedom at the hydraulic ports of the unit from the original number of $3n$ (all members as separate entities) to $2n$.

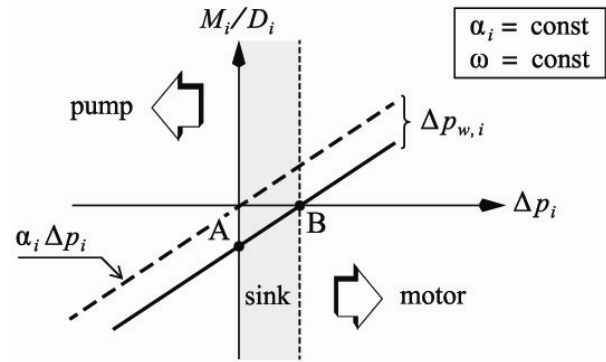


Fig. 2: Working modes according to

A popular implementation with $n = 2$ of the Type A class in aviation is the PTU (Power Transfer Unit) that transfers power from an aircraft's hydraulic system to another in the event that the second has failed or been turned off. Putting aside the informative articles and the patent related documents, the analysis of the device proposed by Watton (2009) is an extremely rare occurrence.

2.2 Type B Class

The CSU Type B class is generated by adding a constraint to the layout of the Type A class; the relevant schematic is shown in Fig. 3. All hydraulic ports located on one side of the unit are connected to a single port by a manifold, whose location (top or bottom) is not important, provided that the virtual setting of all members be allowed to vary in the full range $-1 \leq \alpha_i \leq +1$. Due to the manifold on the opposite side, the multiple ports belong to separate branches of the same circuit.

The new layout implies the link $\Delta p_i = p_{a/b} - p_{b/a,i}$ between the differential pressure terms of Eq. 3. If the positive direction of the flow through the members is the same, Eq. 3 is transformed accordingly to separate the pressure in the input and output ports

$$p_{a/b} \cdot \sum_{i=1}^n D_i \cdot \alpha_i = \sum_{i=1}^n D_i \cdot \alpha_i \cdot p_{b/a,i} + \sum_{i=1}^n D_i \cdot \Delta p_{w,i} \quad (6)$$

irrespective of the global positive direction of the fluid flow (up or down in Fig. 3). If the setting of one or more variable members becomes negative - no matter if the displacement control is bilateral or not - or the set-

ting of a fixed member becomes -1, the local flow is reversed and a recirculation takes place in the manifold.

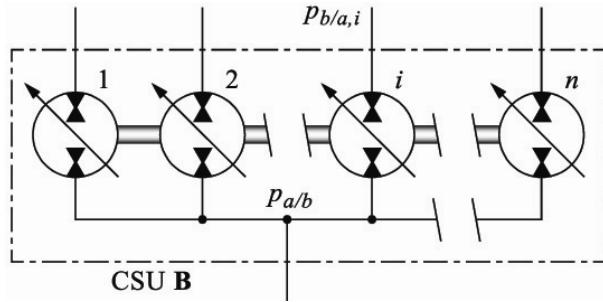


Fig. 3: Schematic of the CSU Type B class

The Type B class shares with Type A the compatibility with any combination of fixed and variable members (all variable and all fixed included). If all members have the same fixed displacement and the same direction of flow (i.e. $\alpha_i = +1$), Eq. 6 is simplified as in Eq. 7:

$$n \cdot p_{a/b} = \sum_{i=1}^n p_{b/a,i} + \sum_{i=1}^n \Delta p_{w,i} \quad (7)$$

Equation 7 makes visible some interesting properties, whose generalized version is also applicable to Eq. 6:

- it confirms the well known result that the pressure in the manifold port is slightly higher than the average of the pressure in the separate ports;
- it states that, if all separate ports are at the same pressure, all members of the unit must be in the idling state. Alternatively, if the generic pressure is $p + \delta_i$ and the small shifts δ_i add to zero¹, the members work close to point B in Working modes according to (some on the right, some on the left).

Since the members of the Type B class units are often externally drain-free, Eq. 4 calculates the flow in the separate ports. Then, the conventional continuity law - i.e. fluid density independent from pressure and temperature - with the same assumptions of Eq. 7 states that

$$\frac{Q_{a/b}}{\omega \cdot D} = n + \sum_{i=1}^n \frac{\text{sgn}(\Delta p_i) + 1}{2} \cdot \frac{\omega_{w,i}}{\omega} \quad (8)$$

The functional degrees of freedom at the hydraulic ports are reduced from the original number of $3n$ (all members as separate entities) to $n + 1$.

Equation 8 explains why the most popular implementation of the Type B class is the volumetric flow divider and/or combiner, often used to approximate the synchronous motion of two or more actuators (up to 10 or more). Other applications, typically with $n = 2$ and one separate port goes to tank, are the pressure or flow intensifiers. Despite the larger use of Type B units, the remark on the literature coverage of the Type A units applies almost untouched to the volumetric flow divider; the paper by Morgan (1991) is representative of the approach².

¹This assures that the pressure in the manifold is immune.

²Curiously, the passive - or throttling based - flow divider/combiner seems to be more seductive to the authors.

2.3 Type C Class

The CSU Type C class is generated by adding two constraints to the layout of the Type A class; the relevant schematic is shown in Fig. 4. Just two external ports are connected to the CSU members by two manifolds and the whole unit appears as a single compound member.

The physical constraints imply that the same Δp is shared by all members and Eq. 3 becomes

$$\Delta p \cdot \sum_{i=1}^n D_i \cdot \alpha_i = \sum_{i=1}^n D_i \cdot \Delta p_{w,i} \quad (9)$$

i.e. a special case of the CSU second rule. Equation 9 hides a paradox revealed by supposing that all members be fixed and the direction of flow be the same (i.e. $\alpha_i = +1$). Since its multiplier is constant, the Δp which satisfies Eq. 9 should be of the same order of the p_{wi} terms and the unit would be practically frozen. To unveil the paradox, the displacement settings must be partly positive and partly negative so that the multiplier of Δp be small enough to allow the increase of the differential pressure.

Due to the symmetry of Fig. 4, once the inflow port is chosen the positive flow direction is fixed. If the high pressure manifold is on the inflow port side and the drains are external (as generally advisable in this class), $\Delta p_i = p_a - p_b$ and the continuity law states that

$$Q_a = \omega \cdot \sum_{i=1}^n D_i \cdot \alpha_i + \sum_{i=1}^n D_i \cdot \omega_{w,i} \quad (10)$$

where the second term is the total drain. The continuity law applied in the low pressure manifold states that

$$Q_b = \omega \cdot \sum_{i=1}^n D_i \cdot \alpha_i - \sum_{i=1}^n D_i \cdot \alpha_i > 0 \quad (11)$$

where the multiplier of ω is positive (Eq. 9). The combination of Eq. 9 and Eq. 10 is (provided that the drains come from the high pressure side) the overall power balance

$$\Delta p \cdot Q_a = \omega \cdot \sum_{i=1}^n D_i \cdot \Delta p_{w,i} + \Delta p \cdot \sum_{i=1}^n D_i \cdot \omega_{w,i} \quad (12)$$

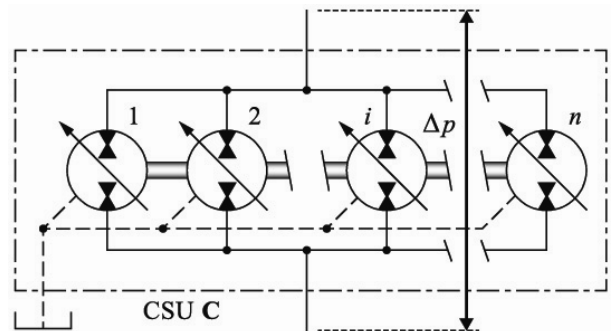


Fig. 4: Schematic of the CSU Type C class

Literally, Eq. 12 means that the entering power compensates the internal losses of the CSU members. Conceptually, it means that the Type C class - differently from the true fluid power components, which work despite their power losses - makes sense thanks to its power losses. In other words, the interest of Type A

and B lies on what happens outside the CSU, but the interest of Type C lies on what happens inside the CSU.

2.4 Type X Class

If some members of a Type A CSU are replaced by as many Type C CSUs, a particular Type X class is generated and its analysis is a combination of the individual ones. Disregarding the intermediate results, the corresponding form of Eq. 12 becomes

$$\omega \cdot \sum_{j=1}^r M_j + \sum_{i=1}^s Q_{a,i} \cdot \Delta p_i = \sum_{i=1}^s P_{w,i} \tag{13}$$

being r the residual size of the Type A CSU and s the number of the Type C CSUs. Equation 13 means that the power losses of the latter ones are also compensated by the combined torque of the Type A units (if positive).

2.5 Further Steps

If the previous discussions are focused on what the various CSU classes actually do, the investigation of how they do should resort to the wide variety of simulation tools, from the simplified closed form analysis to the numerical nonlinear dynamics (virtual experiments).

The good point to start with is the Type C class (treated in Section 3) because it's less popular than the B class, less prestigious than the A class, and suitable of customized implementations. As a complement, the Type X class is treated (more briefly) in Section 4.

3 Flow Compensation

The minimum Type C unit requires $n = 2$, which means that the common shaft connects one pump and one motor (first CSU rule). The variable displacement is ascribed to the pump because it's more representative of the commercial offer than a variable motor. In principle, the scheme is easily expanded to a group of pumps (at least one of them variable) and a group of motors, but in practice this option has more cons than pros³.

The translation of the CSU concept into a workable system generates a (rotary) regenerative circuit, to mark the difference from the homonymous cylinder operation. By nature, its only mission is to keep running the two units, which turns out to be beneficial to their laboratory testing - specially fatigue and/or cycling - because it's: (a) relatively simple and ease to monitor, even for long periods; (b) energy saving, if the input power is lower than the shaft power; (c) highly flexible, because pressure and speed can be moved within the expected operating envelope of the units, even forcing their boundaries.

The capabilities of the assembly are expanded by replacing the shaft with a passive component, e.g. a

gearbox (Feng et al., 2010). Though the analysis must be adapted, the advantages are substantially preserved.

3.1 Regenerative Circuit

The regenerative circuit is shown in Fig. 5, where the relevant nomenclature is intentionally adapted to the physical meaning.

In the low pressure line the excess flow Q_c - at least equivalent to Q_b in Eq. 11 - is positive, and the convenient condition $p_0 \approx \text{const}$ is easily met by a relief valve (some kind of an embedded boost). In the high pressure line, the compensating flow Q_c should come from a variable displacement pump driven by a separate prime mover. The high pressure is variable and affects the overall $\Delta p = p - p_b$ accordingly.

A real circuit will deserve the proper precautions intended to reduce the power losses in pipes or tubes and to improve the dynamics (rotational inertia as small as possible). But the feasibility relies mostly on the size of the members, as proved by the upper bound of the differential pressure derived from Eq. 9:

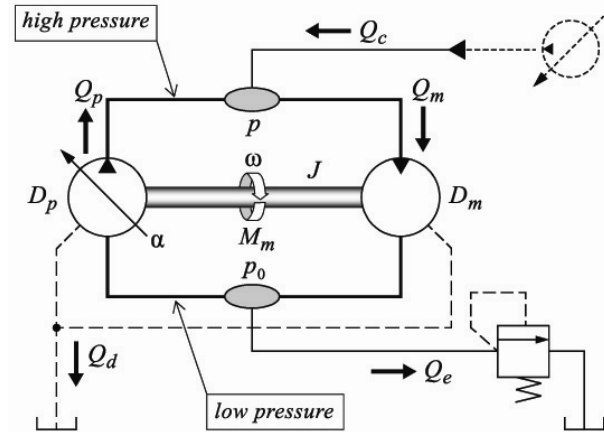


Fig. 5: Regenerative circuit (flow compensated)

$$\frac{k \cdot \Delta p_{w,m} + \Delta p_{w,p}}{k - \alpha} \tag{14}$$

where $k = D_m / D_p$ is the size ratio. Since the designer, who is surely interested in getting high pressure levels, does not command the equivalent losses, three solutions are available, depending on his/her freedom of choice:

- the maximum confidence is granted if k is equal or slightly less than 1 because the denominator of Eq. 14 can be always made as small as necessary;
- if the k ratio is higher than 1 (but not too much) the situation is at risk because it's not sure that even $\alpha = 1$ be enough;
- if the k ratio is significantly different from 1, a speed adapter should be inserted between the members to get back to the $k \approx 1$ ratio. The reverse approach is necessary if the adapter itself is under test.

Though the above guidelines might come in handy to design a real circuit, the $k = 1$ (or $D_p = D_m = D$) specification is assumed in the continuation of the paper.

³A sure advantage of two members is the mechanical design, because they can be mounted face to face.

3.2 Steady State Performance

The steady state performance of the circuit of Fig. 5 obeys two laws: the torque balance in the common shaft, and the flow balance in the high pressure line. The first comes straight from Eq. 9

$$1 - \alpha = \frac{\Delta p_{w,p} + \Delta p_{w,m}}{\Delta p} \quad (15)$$

The second law requires the preliminary calculation of the flow displaced by the pump and the flow received by the motor. Both can be included in the same definition

$$Q_{p/m} = \omega \cdot D \mp D \cdot \omega_{w,p/m} \quad (16)$$

where the flow losses are defined as in Eq. 4 or Eq. 5 and the minus sign applies to the pump. Consequently, the flow balance is expressed as follows

$$\frac{Q_c}{\omega \cdot D} = 1 - \alpha + \frac{\omega_{w,p} + \omega_{w,m}}{\omega} \quad (17)$$

which is ready to receive the result of Eq. 15. The significant title of merit of the circuit is the compensation index I_c defined as the ratio between the hydraulic power supplied from the outside and the mechanical power transmitted by the shaft. Given the conventional definition of the total efficiency as product of the partial volumetric and hydromechanical efficiencies (derived from the flow and torque losses)

$$I_c = \frac{Q_c \cdot p}{\omega \cdot M_s} = \left[1 + \frac{p_0}{\Delta p} \right] \cdot \left[\frac{1}{\eta_{t,m}} - \eta_{t,p} \right] \quad (18)$$

Though the effect of the boost pressure p_0 is not to be ignored⁴, the most interesting part of Eq. 18 is the partial factor that depends on the total efficiency of the volumetric machines, i.e.

$$I_{c,0} = 1 / \eta_{t,m} - \eta_{t,p} \quad (19)$$

Granted that the sensitivity of $I_{c,0}$ to the motor efficiency is higher than the sensitivity to the pump efficiency - as proved by the partial derivatives - its 3D plot is shown in Fig. 6. The surface is divided in two parts by the isolevel curve at $I_{c,0} = 1$. In principle, this threshold would be the upper bound of regeneration, but in practice the decisive factor is not the index in itself but its combination with the shaft power, because the concern of the designer is focused on the maximum power available outside: if the shaft power is small - e.g. 3 kW - even a global compensation index of 2 or 3 is acceptable. Moreover, the occasional expenditure of few additional kW is negligible if compared with the saving attained when the index is low and the power is high.

3.3 Dynamic Performance

The simplest dynamic model of the circuit of Fig. 5 is just an extension of Eq. 15 and Eq. 17 got through the

⁴The boost pressure is decisive at high shaft speeds.

⁵Truly, the conclusion is mainly speculative because in most cases the equivalent inertia of the transmission motor is higher than the inertia of the regenerative circuit.

addition of the time derivatives of pressure and speed

$$\begin{cases} \frac{J}{D} \cdot \frac{d\omega}{dt} = (1 - \alpha) \cdot \Delta p - \Delta p_{w,p} - \Delta p_{w,m} \\ \frac{V}{B \cdot D} \cdot \frac{dp}{dt} = Q_c + (\alpha - 1) \cdot \omega - \omega_{w,p} - \omega_{w,m} \end{cases} \quad (20)$$

By performing a conventional linear analysis and choosing the position $p \approx \Delta p$ plus the following assumptions about the functional dependence of the losses

$$\frac{\partial \sum \Delta p_w}{\partial p} = \frac{\partial \sum \omega_w}{\partial \omega} = \frac{\partial \sum \Delta p_w}{\partial \omega} \cdot \frac{\partial \sum \omega_w}{\partial p} \approx 0$$

the natural frequency and the damping ratio of the circuit of Fig. 5 turn out to be

$$f_{CSU} = (1 - \alpha) \cdot f_{HT} \quad \zeta_{CSU} = \frac{\zeta_{HT}}{1 - \alpha} \quad (21)$$

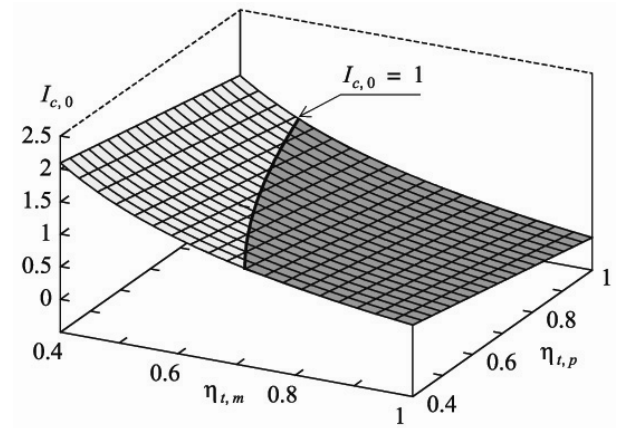


Fig. 6: Plot of the compensation index (partial)

Where the subscript HT refers to a hydrostatic transmission assembled with the members of Fig. 5 and the pump driven at constant speed. Since $(1 - \alpha)$ is a relatively small term (as shown by Eq. 15), the mechanical link between pump and motor in the regenerative circuit causes a drastic change of the dynamic properties⁵.

3.4 Operation Modes

The operating modes of the circuit of Fig. 5 are detectable if the losses in Eq. 15 and 17 are replaced by the partial efficiencies (volumetric and hydromechanical) which depend on setting, speed and differential pressure. For a given size of the volumetric machines, the four unknown quantities can be grouped in two subsets: speed and differential pressure (the reaction variables), the setting and the compensating flow (the action variables). In Fig. 7 two scenarios are depicted:

- if the reaction variables are inputs and the action variables are outputs (from right to left), the mathematical solution of the two implicit equations does not point to a valid operating mode;
- if the action variables are inputs and the reaction variables are outputs (from left to right), the mathematical solution points to a sound operating mode.

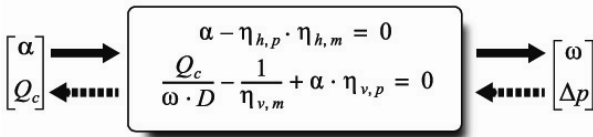


Fig. 7: Solution of the steady state laws

Actually, two operating modes are feasible. In the open mode the action variables are set independently; in the closed mode the action variables are set automatically on the basis of the desired values of the reaction variables.

3.5 Simulation Model

Being no “universal model” of the flow and torque losses agreed upon by the scholars, and considering the explanatory purpose of the simulation, the model used here was originally developed by the author to look into the hydrostatic transmissions, having in mind a relatively simple tool, able to accommodate some generally accepted trends and cover three issues: the separation of external and internal flow losses, the functional inversion (not interesting here) and the rise of the torque losses in the low speed range (at constant pressure).

The volumetric machines are modeled as components with three external ports - named 1, 2 (power ports) and 3 (drain) - whose flow rates are described by a bilateral extension of the Wilson model (Wilson, 1948):

$$\begin{cases} \frac{Q_1}{Q_n} = -\alpha \cdot \bar{\omega} - c_1 \cdot \bar{p}_1 + c_3 \cdot \bar{\Delta p} \\ \frac{Q_2}{Q_n} = \alpha \cdot \bar{\omega} - c_2 \cdot \bar{p}_2 - c_3 \cdot \bar{\Delta p} \\ Q_1 + Q_2 + Q_3 = 0 \end{cases} \quad (22)$$

where the nominal flow $Q_n = D\omega_n$ is always positive ($\omega_n = 4000$ rpm) and $p_2 - p_1 = \Delta p$. Given a positive rotation of the shaft, the flow is positive when leaving and negative when entering the component. The model fits both pumps ($\bar{\omega} \Delta \bar{p} > 0$) and motors ($\bar{\omega} \Delta \bar{p} < 0$)⁶.

The same rationale is behind the torque loss model, i.e. a positive torque is produced by and a negative torque is applied to the component. They are described by an expression partly inspired by a much more detailed model for transmission units (Rydberg, 1983)

$$\frac{M}{M_n} = -\alpha \cdot \bar{\Delta p} - c_4 \cdot \bar{\omega} - \frac{c_5 + \frac{c_6}{1 + \bar{\omega}/c_7}}{|\bar{\omega}|} \cdot [\bar{p}_1 + \bar{p}_2] \quad (23)$$

where the nominal torque $M_n = D p_n$ is always positive and $p_n = 4000$ bar. The dimensionless coefficients listed in Table 1 have been derived by fixing the losses in the nominal states (e.g. the external drain is about three times the internal drain); they produce relatively high efficiencies, useful to highlight the sensitivity of the system. The displacement of the CSU members is 50 cc/rev and the total shaft inertia is 0.015 kg/m² (the

⁶The sink mode is omitted for the sake of simplicity.

displacement justifies both inertia and nominal speed); the setting of the variable member follows an external directive through a first order block (time constant of 0.1 s), both position and rate limited. The same model applies to the external pump of 70 cc/rev, rotating at 1500 rpm constant. The CSU members are connected by two pipes of 1 m length and 20 mm diameter, for a total volume of about 400 cc each.

Table 1: Loss coefficients (Eq. 22 and 23)

c1	c2	c3	c4	c5	c6	c7
0.015	0.005	0.035	0.015	0.1	0.05	

The last piece of hardware is the relief valve, described by a first order model (time constant of 0.01 s) set at 15 bar; in operation the pressure gets a maximum of about 20 bar.

The whole system is assembled and solved in the Easy5 simulation environment (MSC, 2010).

3.6 Open Mode Operation

In the open mode operation the external pump is omitted to enhance the compatibility with the analysis of Section 3.2. The compensating flow and the pump setting are the inputs, while high pressure, shaft speed and shaft power are the relevant outputs. The steady state solutions are approximated by running slow dynamic cycles (40 s) with constant setting and variable flow.

In Fig. 8 the shaft speed and the differential pressure (both dimensionless) - sometimes exceeding the nominal levels - are plotted against the compensating flow; the pressure curves (dotted) are affected by the hysteresis of the inertia torque, amplified by the factor (1 - α). The left ends are explained in Fig. 10.

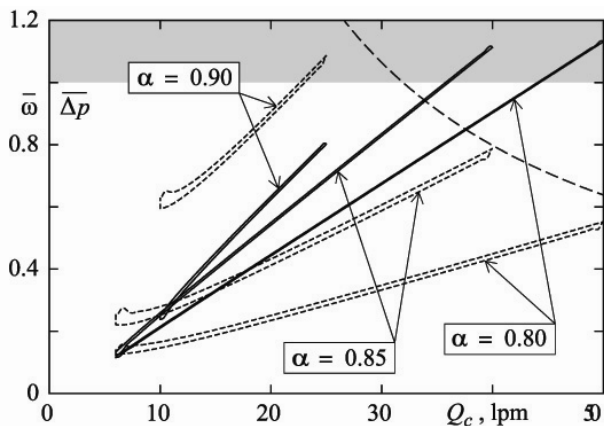


Fig. 8: Speed and differential pressure vs Q_c flow

In Fig. 9 the shaft power - ratioed to the nominal power of 133.3 kW - and the compensation index (calculated according to Eq. 18) are plotted vs. the compensating flow. The power plots (dotted) increase with flow and setting; conversely, the compensation index plots decrease as flow and setting increase. A rough estimate of the relationship between the compensation index and the shaft power, is helped in Fig. 8 by the hyperbole that touches the right end of the intermediate pressure plot.

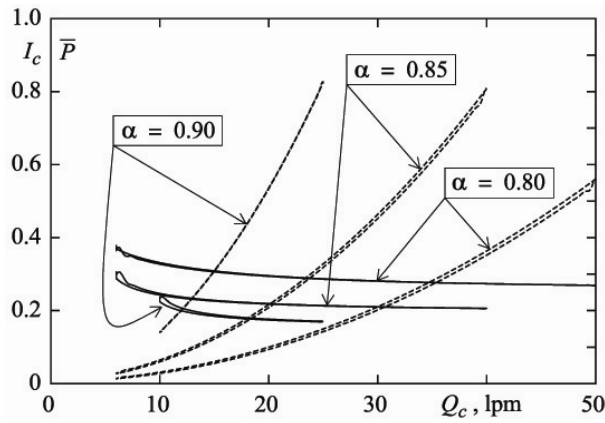


Fig. 9: Shaft power and I_c index vs Q_c flow

Figure 10 shows how the reaction variables move in the operation plane. These plots justify the lower limit of the flow range: in fact, the simulation cycles go close to or overlap the dotted curve that estimates the position of the maximum motor (and minimum pump) torque

$$\bar{\Delta p} = \frac{c_4 \cdot c_7}{c_6} \cdot \left[1 + \frac{\bar{\omega}}{c_4} \right] - 2 \cdot \frac{p_0}{p_n} \quad (24)$$

In the grey area of Fig. 10 the torque balance of the shaft is unstable and the steady state operation is impossible.

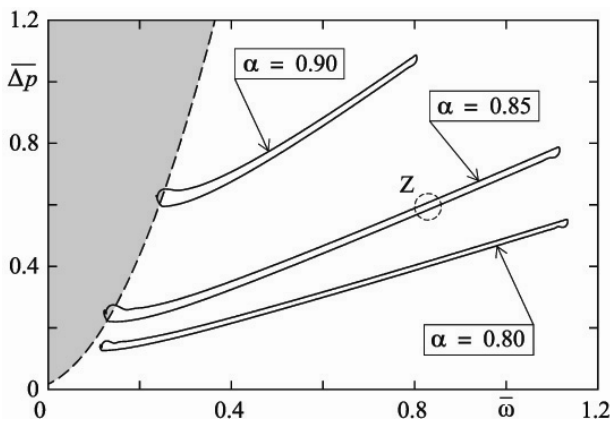


Fig. 10: Operation plane of the reaction variables

If the method of Fig. 8 would be repeated systematically to map the operation plane with a full grid of the action variables, the pump setting and the compensation flow could be scheduled to follow a trajectory of interest. Such an approach has some advantages - first of all, it's simple - but its drawbacks are clear as well: limited accuracy, extensive preliminary testing, and sensitivity to any alteration of the member losses⁷.

3.7 Closed Mode Operation

In the closed mode operation the pump setting and the compensating flow are generated by an automatic

⁷The last assessment would be revised if the regenerative testing would use the drift of the reaction variables as a symptom of any changes of the efficiencies (Fig. 7).

⁸One of the various "eight-shaped" curves.

process whose inputs are the desired shaft speed and differential pressure. The approach is not as simple as the open mode, but its advantages are tempting: the accuracy is improved, the preliminary testing reduced and the sensitivity to the hardware degradation minimized.

The job would require a DIDO (Double Input Double Output) control, i.e. a particular multivariable control, a tentative prototype of which was already tested (Zarotti, 1989). Before dealing with such a tool, it's customary to estimate "a priori" the amount of interaction between the action and reaction variables. The relative gain method (Doebelin, 1985) is relatively easy to use and can be performed by the same simulation model. The relevant gain matrix - its properties are summarized in the Appendix - is computed in the region Z of Fig. 10 and the results shown in Table 2 (the high pressure replaces the differential pressure, as explained later). Two conclusions are legitimated by the method:

- a certain amount of interaction exists because the diagonal terms are greater than 1;
- if a genuine DIDO is tentatively replaced by two SISO (Single Input Single Output) control loops, the setting loop should control the pressure and the speed loop should control the flow.

Table 2: Relative gain matrix (region Z of Fig. 10)

	α	\bar{Q}_c
\bar{p}	1.387	-0.387
$\bar{\omega}$	-0.387	1.387

According to the latter conclusion, the operation of the regenerative circuit is demonstrated by two SISO controls based on the PID strategy with the same gains: 10, 8 and 0.2: one acting on the setting of the internal pump, the other acting on the setting of the external pump that comes into play as source of the compensating flow. While tuning the gains, two expedients were necessary to get a stable response of the overall system:

- the true differential pressure feedback is replaced by the difference between the high pressure p and 16.5 bar (a conventional average of the low pressure);
- any flow exchange of both displacement control circuits with the high pressure line is precluded.

Since the control design is not the prevailing aim of the paper, the strength of these constraints is open to future evaluations because they might depend on the simplified control scheme and/or the nature of the test cycles.

3.8 Test Cycles

The dynamic simulation is based on a reference trajectory defined in terms of speed and pressure. The trajectory is a lemniscate of Geron⁸ with variable origin and variable pitch in the operation plane of Fig. 10. Its two-dimensional parametric form is the following

$$\begin{cases} x = a + s \cdot \cos\theta \cdot \cos\varphi - s \cdot \sin\theta \cdot \sin 2\varphi \\ y = b + s \cdot \sin\theta \cdot \cos\varphi + s \cdot \cos\theta \cdot \sin 2\varphi \end{cases} \quad (25)$$

where x and y are the generic coordinates, (a, b) is the origin of the curve, s the scale factor (the same in both directions), θ the pitch angle (positive if counterclockwise), and $\varphi = 2\pi f t$ the parametric variable. The data used in two simulated cycles are collected in Table 3.

Table 3: Parameters of the test cycles

CYCLE	a	b	s	θ
# 1	0.7	0.5	0.3	20 °
# 2	0.5	0.7		

The cycle of Eq. 25 belongs to the family of the “space driven” cycles because their main purpose is to cover a portion of the operation plane⁹. Conversely, the “time driven” cycles, typically used in the long run or fatigue testing, are set up as a sequence of speed or pressure steps, i.e. they become segments parallel to the x - or y -axis in the operation plane.

3.9 Simulation Results

The performance of the regenerative circuit driven by cycle # 1 is shown in the operation plane of Fig. 11. The frequency is 0.1 Hz, which means that a complete lemniscate is completed in 10 seconds, though the plots are limited to 9.5 seconds to improve their visibility: the dotted plot is the reference pattern and the solid plot is the response pattern. During the experiment the internal pump setting ranges between 0.67 and 0.90 with a maximum rate of change of about 0.24 s⁻¹, while the external pump setting ranges between 0.14 and 0.60 with a maximum rate of change of about 0.35 s⁻¹. This raises the problem of the proper size of the external pump, which is a compromise between three contrasting requirements: in fact, the displacement should

- be small enough to allow the setting to be high and to preserve the efficiency of the component;
- be high enough to avoid saturation (i.e. $\alpha = 1$) everywhere in the practicable operating plane;
- maintain the above prerogatives when the size or the characteristics of the CSU members change.

A tentative trade-off might be a variable speed drive of the pump and/or the combination of more pumps.

The assessment of the experiment is shown in Fig. 12 from two viewpoints. The upper plot accommodates the overall or total compensation index $I_{c,t}$ between the shaft power of the external pump and the internal shaft power, during the first lap. The maximum of 0.77 is located at medium speed and low pressure (i.e. low power). The lower plot accommodates the local compound error, defined as the distance between a point of the reference pattern and the point of the response pattern at the same time (still during the first lap)

$$e = \sqrt{\left| \frac{\Delta p - p_{ref} + 16.5}{p_n} \right|^2 + \left| \frac{\omega - \omega_{ref}}{\omega_n} \right|^2} \quad (26)$$

where the pressure is measured in bar. The minimum error is measured at the beginning of the cycle (1 %); in the dynamic pattern it ranges between 2 and 8.5 %.

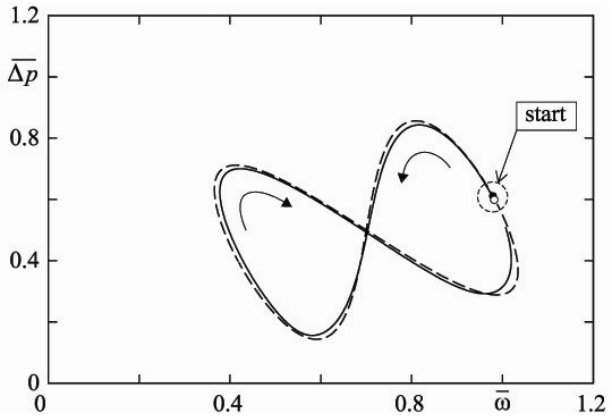


Fig. 11: Simulation results (cycle # 1)

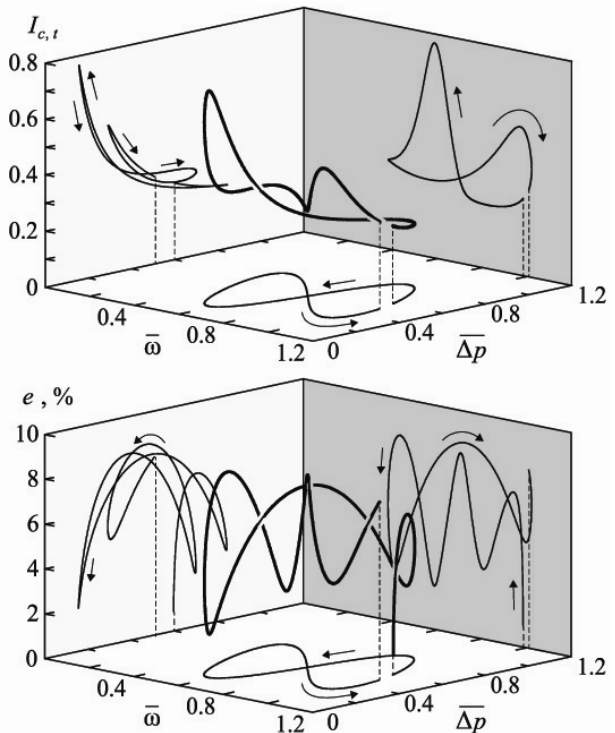


Fig. 12: Assessment of cycle # 1

The performance of the circuit driven by cycle # 2 is shown in Fig. 13. The reference pattern (not plotted) is a shift of cycle # 1 with the same frequency of 0.1 Hz and is partly overlapped with the region bound by the curve of Eq. 24. As the grey region is approached, a significant ripple disturbs the response; but the control survives and, as the cycle leaves the grey region the ripple fades away. The impact of the perturbation is stronger inside the control, causing large and fast fluctuations of the settings: the external pump ranges between 0.01 and 0.31, while the internal pump between 0.80 and 1.00 (i.e. saturation). More impressive are the rates of change, that jump between the ± 20 bounds set in the pump model).

⁹Another example would be a spiral pattern starting or ending in the center of the operation plane.

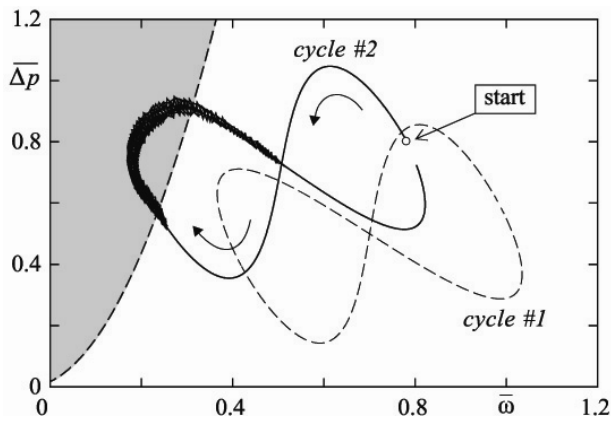


Fig. 13: Simulation results (cycle # 2)

4 The Torque Compensation

The minimum Type X (A + C) class requires, according to Eq. 13, $r = s = 1$ and a minimum Type C unit. Granted that the torque generator might be different from a hydraulic motor (e.g. an electric motor or an i.c. engine) and must comply in any case with the whole speed range of the shaft, the torque compensation can be exploited in two different ways:

- to assist the flow compensation, i.e. modify the circuit of Fig. 5. Possible goals are: (a) extend the test capabilities beyond the power limits of the external pump; (b) provide a bias to make the test bench compatible with a larger pump; (c) provide a degree of freedom to make the test bench compatible with two fixed displacement units;
- to replace the flow compensation, i.e. generate the alternative regenerative circuit of Fig. 14. The main differences from Fig. 5 are: (a) the effective pump displacement is larger (not lower) than the motor displacement; (b) the low pressure line is no longer boosted automatically but requires an input flow (like a conventional hydrostatic transmission).

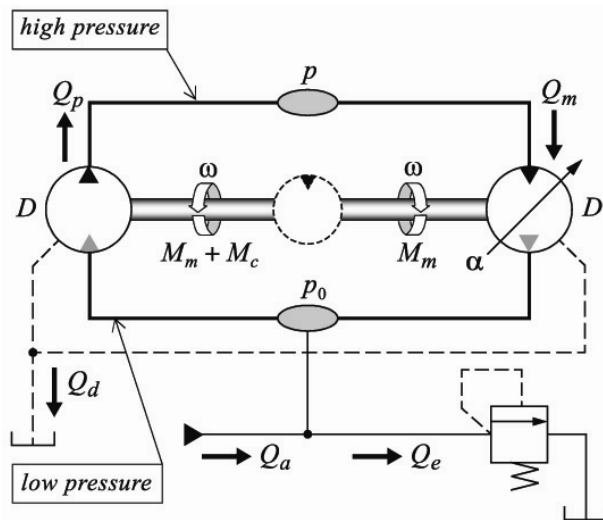


Fig. 14: Regenerative circuit (torque compensated)

In Fig. 14 the motor displacement is variable to remark that the new circuit offers the opportunity to host the same units of Fig. 5 in their reverse operation (the

pump working as “motor” and the motor working as “pump”).

4.1 Steady State Performance

The laws of the steady state performance (torque balance and flow balance) become the following

$$\begin{cases} \frac{M_c}{\Delta p \cdot D} = \frac{\Delta p_{w,p} + \Delta p_{w,m}}{\Delta p} + 1 - \alpha \\ 1 - \alpha = \frac{\omega_{w,p} + \omega_{w,m}}{\omega} \end{cases} \quad (27)$$

An intrinsic property of the circuit of Fig. 14 is that the compensation index - ratio between external and internal power - does not have a unique definition because two preliminary decisions must be taken:

- as to the internal power, the choice between the motor torque and the pump torque;
- as to the external power, whether the term $Q_c p_0$ (i.e. the boost power) should be included or not.

To help the comparison with the flow compensated circuit of Fig. 5, the boost power is neglected and consequently the alternative definitions of the index are

$$I_{c,1} = \frac{1}{\eta_{t,m} \cdot \eta_{t,p}} - 1 \quad I_{c,2} = 1 - \eta_{t,m} \cdot \eta_{t,p} \quad (28)$$

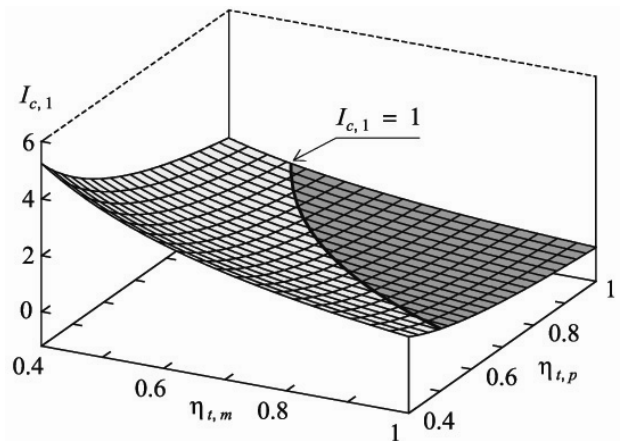


Fig. 15: Plot of the compensation index (motor based)

The left index, based on the motor torque, is plotted in Fig. 15, to be compared with the surface of Fig. 16. As the efficiencies of the volumetric machines decrease, the index becomes much higher and consequently the region confined by the isolevel curve located at $I_{c,1} = 1$ is smaller, the torque compensated circuit seems less favorable. However, if the right index of Eq. 28 is adopted¹⁰, the torque compensated circuit seems more favorable because the compensation index is always less than one.

¹⁰Some people are convinced that the compensation index be in all regenerative circuits.

5 Conclusion

The systems collected under the general label of Common Shaft Units (CSUs) are supported by a lively concept which is able to generate a multiplicity of circuits. Some applications of the CSUs already exist but it's reasonable to expect many more if the potential of the concept would be steadily included in the repository of the design resources.

One CSU class in particular offers two regenerative circuits, useful to ease the testing of the volumetric machines and making it less expensive. Moreover, they provide a fertile breeding ground for the investigation of multivariable controls.

Nomenclature

c	loss coefficient (dimensionless)
D	cubic displacement
e	error (dimensionless)
f	natural frequency
I	index
J	moment of inertia
M	torque
P	power
\bar{P}	power ratioed to the nominal power
p	pressure
\bar{p}	pressure ratioed to the nominal pressure
Δp	differential pressure
$\Delta \bar{p}$	differential pressure ratioed to the nominal pressure
Q	volumetric flow rate
$sgn(x)$	+1 or -1 according to the sign of x
t	time
α	partial displacement (setting) of pump or motor
η	efficiency of pump or motor
ω	rotational speed
$\bar{\omega}$	speed ratioed to the nominal speed
ζ	damping ratio

Subscripts

a	input port (flow in)
b	output port (flow out)
c	compensating or compensation
d	drain
e	excess
h	hydromechanical
m	hydraulic motor
n	nominal
p	hydraulic pump
ref	reference
s	shaft
t	total
v	volumetric
w	loss
a/b	a or b (and similar)

References

- Doebelin, E. O.** 1985. Control System Principles and Design, *John Wiley & Sons*, pp. 552 - 560.
- Feng, J., Zhang, M., Li, Y., Zhao, S., Zhu, C., Sun, Y. and Zhang, F.** 2010. Energy-saving rotary fatigue test device, Patent CN 201637565 (in Chinese).
- Hornby, A. S.** 1974. Oxford Advanced Learner's Dictionary of Current English, *Oxford University Press*, 3rd Edition, p. 593.
- Leati, E., Marani, P., Ansaloni, G., and Paoluzzi, R.** 2010. Active Regeneration Load Sensing: a simulated comparison with traditional load sensing system in excavator working cycle, *Proc. of the 7th International Fluid Power Conference*, Aachen. Vol I, pp. 103 - 115.
- Morgan, G.** 1991. Gerotor rotary flow dividers, *The American Society of Agricultural Engineers*, Paper N. 911596, pp. 1 - 27.
- MSC** 2010. EASY5 2010 Reference Manual, *MSC Software Corporation*.
- Rydberg, K.-E.** 1983. *On performance optimization and digital control of hydrostatic drives for vehicle applications*, Linköping Studies in Science and Technology, Dissertations, N. 99, Linköping University.
- Watton, J.** 2009. Fundamentals of Fluid Power Control, *Cambridge University Press*, pp. 183-189.
- Wilson, W. E.** 1948. Performance criteria for positive displacement pumps and fluid motors, *ASME Semi-annual Meeting*, Paper 48-SA-14, American Society of Mechanical Engineers.
- Zarotti, G. L.** 1989. Rotary regenerative assemblies - Operation and control, *Proc. of the 2nd International Conference "Fluid Power Transmission and Control"*, Hangzhou (RPC), pp. 355 - 360.
- Zarotti, G. L.** 2001. Load Sensing - cronaca di una testarda giovinezza, *Oleodinamica e Pneumatica*, Vol. XLII, N.3, pp. 130 - 137.

Appendix

Given a system having the outputs y_1 and y_2 and the inputs u_1 and u_2 the local dependence of the former from the latter in a steady state condition is

$$\begin{cases} dy_1 = B_{11} \cdot du_1 + B_{12} \cdot du_2 \\ dy_2 = B_{12} \cdot du_1 + B_{22} \cdot du_2 \end{cases} \quad B_{ij} \equiv \left. \frac{\partial y_i}{\partial u_j} \right|_{u_{k \neq j} = \text{const}} \quad (29)$$

where the coefficients B_{ij} are the elements of the open loop gain matrix, easily extended to multiple inputs and outputs. If a closed loop control is active between u_2 and y_2 and its effect is to force $dy_2 = 0$ a new coefficient or gain is calculated from Eq. 29

$$D_{11} = \frac{B_{11} \cdot B_{22} - B_{12} \cdot B_{21}}{B_{22}} = \left. \frac{\partial y_1}{\partial u_1} \right|_{y_2 = \text{const}} \quad (30)$$

With a similar method, three more D gains can be calculated in a 2 inputs and 2 outputs system. The extension of the D gains to multiple inputs and outputs is

$$D_{ij} \equiv \left. \frac{\partial y_i}{\partial u_j} \right|_{y_{k \neq j} = \text{const}} \quad (31)$$

Now the elements λ_{ij} of the relative gain matrix are defined and calculated on the basis of the \mathbf{B} matrix only, whose estimation is much easier to obtain from either real or virtual experiments

$$\lambda_{ij} = \frac{B_{ij}}{D_{ij}} = B_{ij} \cdot C_{ij} \quad \mathbf{C} = (\mathbf{B}^{-1})^T \quad (32)$$

The fundamental properties of the relative gain matrix, which can be helpful in the choice of separate control loops, are the following (Doebelin, 1985):

- all rows and columns add to 1.0;
- negative gains indicate difficult control problems and the relative pairs should not be used;
- if all gains are of the same magnitude (e.g. 0.5 in a 2 x 2 matrix) the method does not help the decision.

In any case the performance quality of separate control loops depends on their actual architecture and design.



Luca G. Zarotti

Born on November 20th 1945 in Parma, he received the Degree in Aeronautical Engineering at the Polytechnic Institute of Torino (1970). In 1971 he joined the Institute for Agricultural and Earthmoving Machines of the National Research Council of Italy (CNR), where he is still working. He was Director of the same Institute from 2002 to 2009. He had in charge the fluid power course at the Polytechnic Institute of Torino (from 1979 to 1982) and the University of Modena & Reggio E. (from 1996 to 1999). Currently, he is teaching fluid power modeling at the University of Ferrara (from 2002). His research interests cover various aspects of hydrostatic locomotion, displacement control of pumps and motors, load sensing and flow sharing systems for mobile applications. Besides a number of papers and articles, he is the author of three monographs on fluid power fluids (2006), fluid power circuits (2006 and 2010) and hydrostatic transmissions (2010).